

AI-65-42

SECOND QUARTERLY PROGRESS REPORT

INVESTIGATION OF CURRENT DEGRADATION PHENOMENON
IN SUPERCONDUCTING SOLENOIDS

OCTOBER 15, 1964 TO JANUARY 15, 1965

L. C. SALTER, Jr.

GPO PRICE \$ _____

CSFTI PRICE(S) \$ _____

Hard copy (HC) 2.00

Microfiche (MF) .50

ff 653 July 65

FACILITY FORM 602	N65 35450	_____
	(ACCESSION NUMBER)	(THRU)
	30	1
	(PAGES)	(CODE)
CR-67190	26	_____
(NASA CR OR TMX OR AD NUMBER)	(CATEGORY)	

CONTRACT NAS8-5356
MARSHALL SPACE FLIGHT CENTER
HUNTSVILLE, ALABAMA

30876

CONTENTS

	Page
I. Introduction	4
II. Critical Current Measurements	5
III. Resistive Upper Critical Field Measurements	18
A. Description	18
B. Discussion	24
IV. Normal State Resistivity	27
V. Summary and Future Plans	29
References	30

TABLE

1. Critical Current, Normal State Resistivity, and Hardness of Ti-22 at. % Nb Alloy for Various Anneals	28
---	----

FIGURES

1. Critical Current Density and Upper Critical Field at 4.2°K for 0.01-in.-Diameter Ti-22 a/o Nb Wire, β -Quenched from 800°C	6
2. Critical Current Density and Resistive Upper Critical Field at 4.2°K for 0.01-in.-Diameter Ti-22 a/o Nb Wire Annealed at 200°C for the Times Shown	7
3. Critical Current Density and Resistive Upper Critical Field at 4.2°K for 0.01-in.-Diameter Ti-22 a/o Nb Wire Annealed at 250°C for the Times Shown	8
4. Critical Current Density and Resistive Upper Critical Field at 4.2°K for 0.01-in.-Diameter Ti-22 a/o Nb Wire Annealed at 300°C for the Times Shown	9
5. Critical Current Density and Resistive Upper Critical Field at 4.2°K for 0.01-in.-Diameter Ti-22 a/o Nb Wire Annealed at 350°C for the Times Shown	10
6. Critical Current Density and Resistive Upper Critical Field at 4.2°K for 0.01-in.-Diameter Ti-22 a/o Nb Wire Annealed at 400°C for the Times Shown	11
7. Critical Current Density and Resistive Upper Critical Field at 4.2°K for 0.01-in.-Diameter Ti-22 a/o Nb Wire Annealed at 450°C for the Times Shown	12

FIGURES

	Page
8. Critical Current Density and Resistive Upper Critical Field at 4.2°K for 0.01-in.-Diameter Ti-22 ^{a/o} Nb Wire Annealed at 500°C for the Times Shown	13
9. Critical Current Density and Resistive Upper Critical Field at 4.2°K for 0.01-in.-Diameter Ti-22 ^{a/o} Nb Wire Annealed at 550°C for the Times Shown	14
10. Critical Current Density and Resistive Upper Critical Field at 4.2°K for 0.01-in.-Diameter Ti-22 ^{a/o} Nb Wire Annealed at 600°C for the Times Shown	15
11. Critical Current Density and Resistive Upper Critical Field at 4.2°K for 0.01-in.-Diameter Ti-22 ^{a/o} Nb Wire Annealed at 650°C for the Times Shown	16
12. Isometric graph of 4.2°K Critical Currents at 30 kG for Ti-22 ^{a/o} Nb as a Function of Annealing Temperature and Time	17
13. Experimental Circuitry, H _r Measurements	18
14. a. Typical SN Transition in Pulsed-Field, Sample No. 9, J = 109 A/cm ²	20
b. Double Transition in Sample No. 5, J = 117 A/cm ²	20
c. Propagation of Normal Region Originating in Solder Joints	20
15. a. Resistive Upper Critical Field at 4.2°K of Ti-22 ^{a/o} Nb as a Function of Annealing Temperature, for Different Annealing Times	21
b. Resistive Upper Critical Field at 4.2°K of Ti-22 ^{a/o} Nb as a Function of Annealing Temperature, for Different Annealing Times	22
16. Resistive Upper Critical Field at 4.2°K of Ti-22 ^{a/o} Nb as a Function of Annealing Time, for Different Annealing Temperatures	23
17. Ti-Nb Phase Diagram	25
18. Upper Critical Field of Ti-Nb at 1.2°K as a Function of Alloy Concentration	26

I. INTRODUCTION

During the reporting period, precipitation annealing of 30 Ti-Nb wire samples was completed, using the process discussed in the First Quarterly Progress Report (AI-64-198). Subsequently, measurements of critical current density (J_c) vs transverse field, upper resistive critical field (H_r), normal-state-resistivity at 4.2°K (ρ_n), and room-temperature resistivity (ρ_f) were completed. Well defined maximums in critical current density and resistive upper critical field were found as a function of annealing temperature; broader ranges of dependence were found for annealing times. Normal state resistivity measurements at 4.2°K (ρ_n) and at room-temperature (ρ_f) are consistent with H_r determinations.

II. CRITICAL CURRENT MEASUREMENTS

Critical current densities of the 30 Ti-Nb annealed wire samples were measured in transverse magnetic fields. All samples were 4-in.-long wires mounted in hairpin fashion and potted in epoxy. Standard J_c vs H measurements were taken in fields up to 30 kG by increasing the sample current in constant fields until the wire went normal.

The resulting J_c vs H curves are shown in Figures 1 through 11 in conjunction with the upper critical field measurements; critical field measurements are discussed in Section III. Each figure shows the results for wire samples annealed at the same temperature for different times. An isometric plot of J_c at 30 kG as a function of annealing time and temperature is shown in Figure 12. From this figure, it is seen that critical current density is more sensitive to annealing temperature than to annealing time. It reaches a well-defined maximum for 350°C heat treatment but only a broad maximum in the annealing time between 300 to 1000 minutes.

Photomicrographs and x-ray diffraction studies are still in progress. These tests are necessary to determine the dependence of J_c on precipitate size, density, and matrix composition. Preliminary results indicate that precipitate density continues to increase after J_c has reached its maximum.

The J_c vs H measurement for sample No. 9 was extended to 75 kG using facilities at ORNL.* This data is shown in Figure 8.

*We particularly thank Dr. W.F. Gauster, Thermonuclear Group, ORNL, for his cooperation and the use of his facilities.

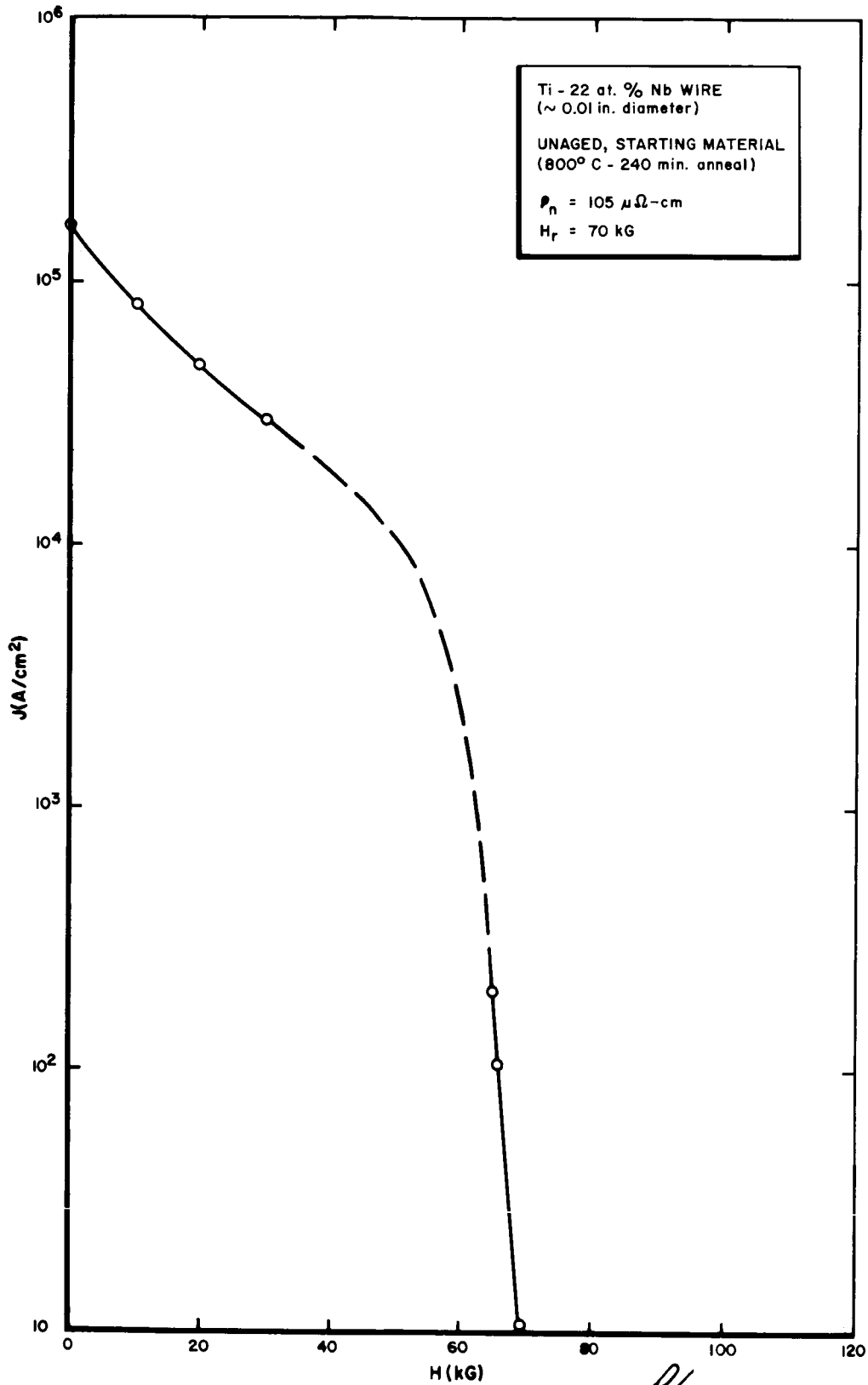


Figure 1. Critical Current Density and Upper Critical Field at 4.2°K for 0.01-in.-Diameter Ti-22 at. % Nb Wire, β -Quenched, from 800° C. This is the Starting Material for Subsequent Anneal

AI-65-42

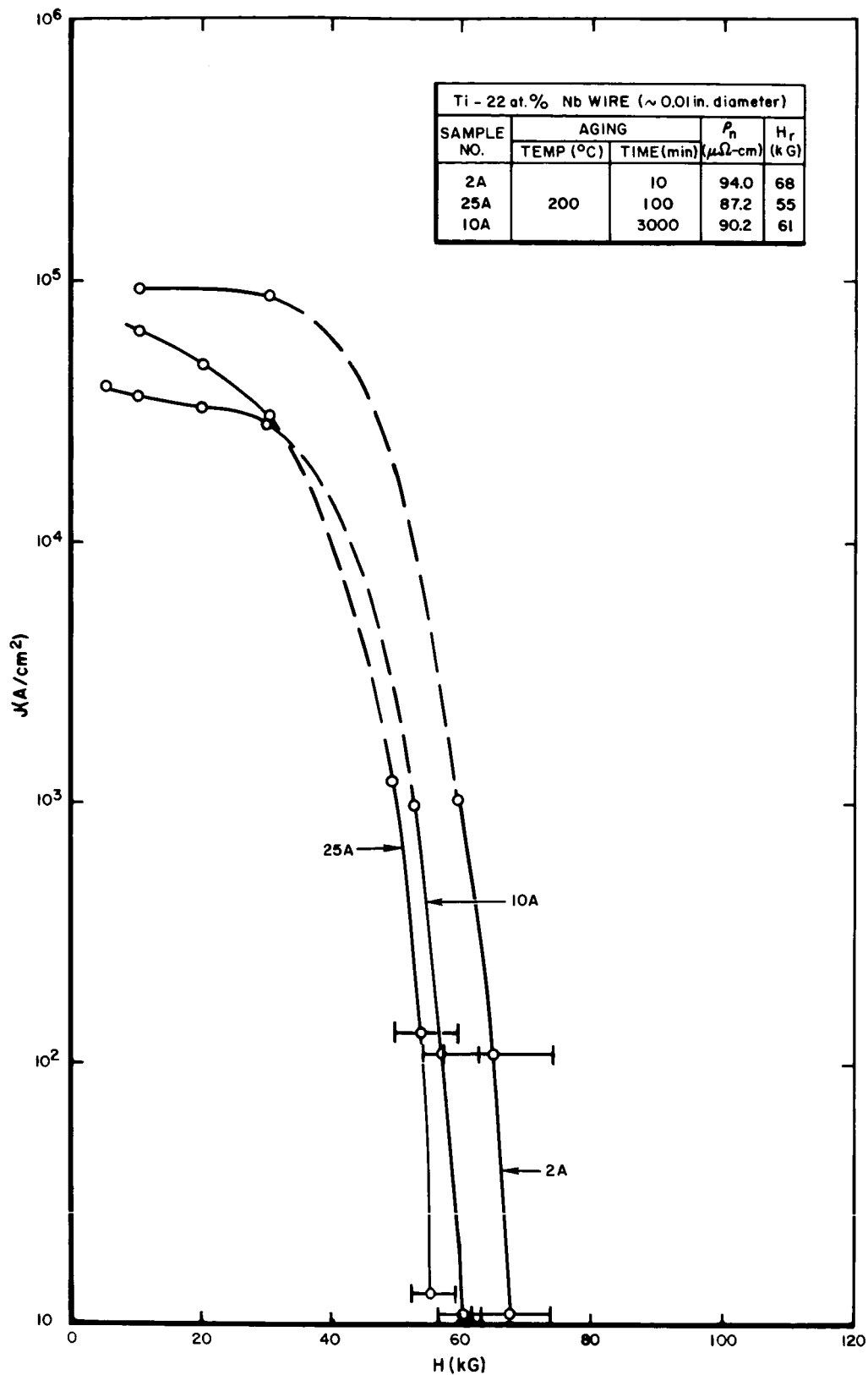


Figure 2. Critical Current Density and Resistive Upper Critical Field at 4.2°K for 0.01-in.-Diameter Ti-22 at.% Nb Wire Annealed at 200°C for the Times Shown

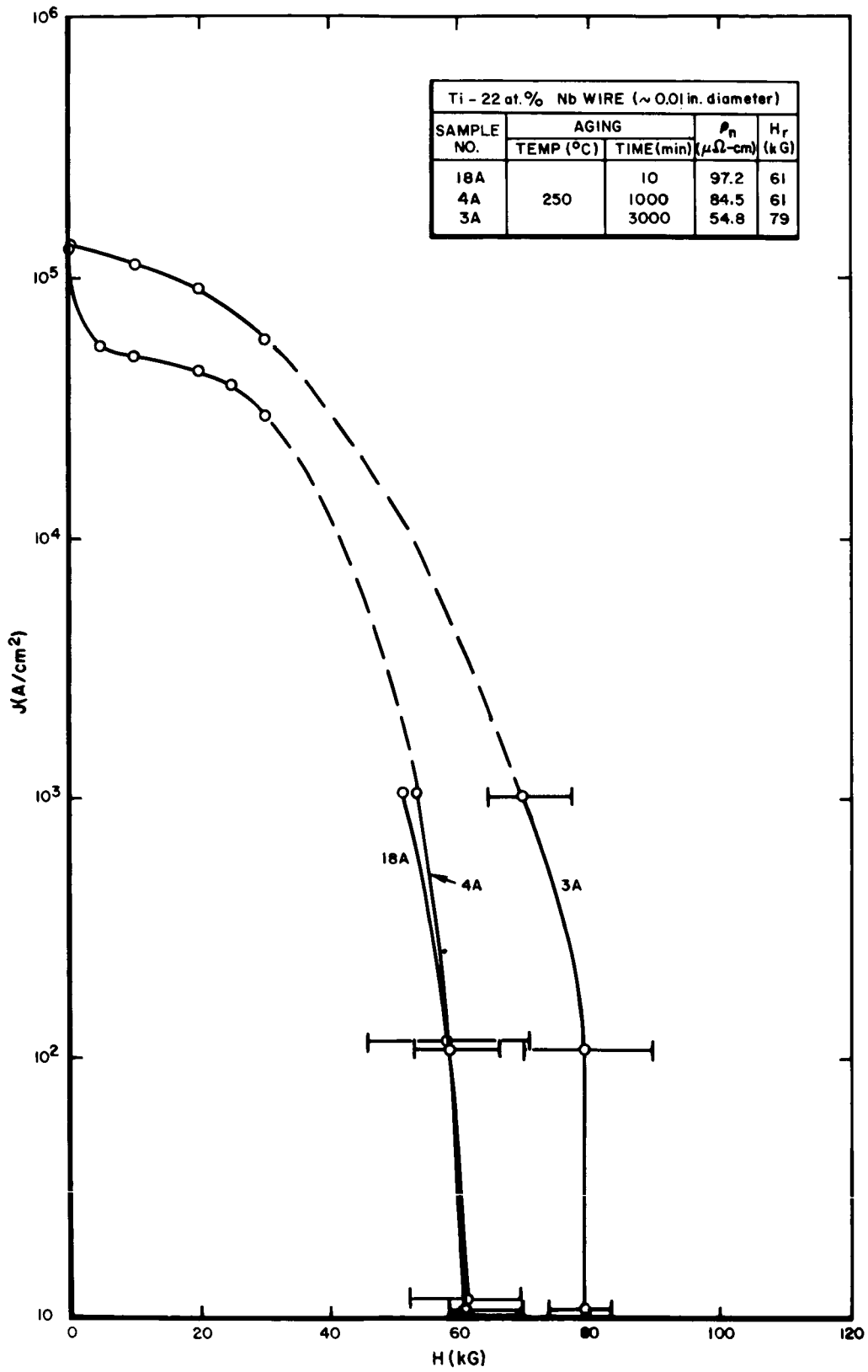


Figure 3. Critical Current Density and Resistive Upper Critical Field at 4.2 °K for 0.01-in.-Diameter Ti-22 at.% Nb Wire Annealed at 250 °C for the Times Shown

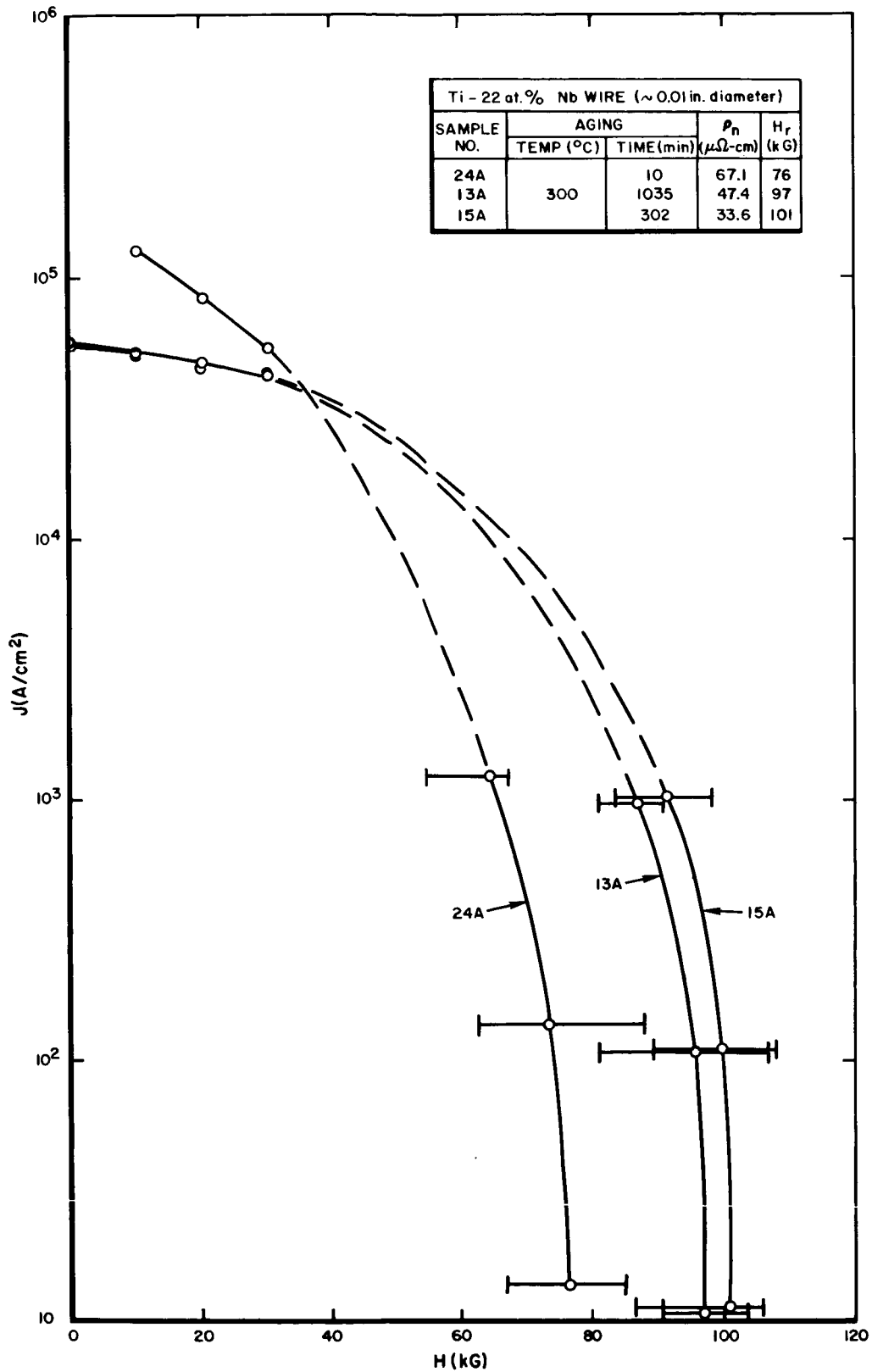


Figure 4. Critical Current Density and Resistive Upper Critical Field at 4.2°K for 0.01-in.-Diameter Ti-22 at.% Nb Wire Annealed at 300°C for the Times Shown

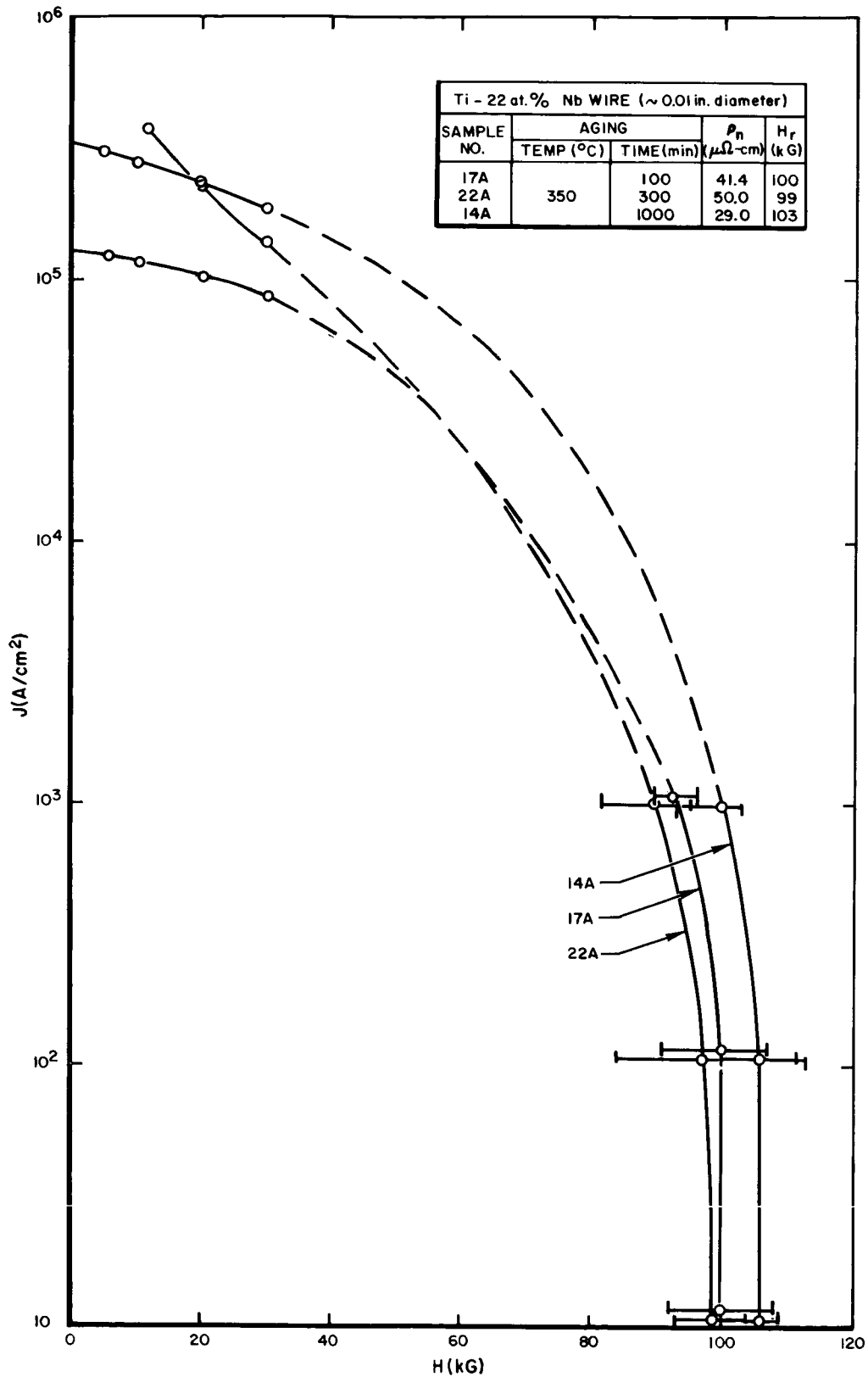


Figure 5. Critical Current Density and Resistive Upper Critical Field at 4.2°K for 0.01-in.-Diameter Ti-22 at.% Nb Wire Annealed at 350°C for the Times Shown

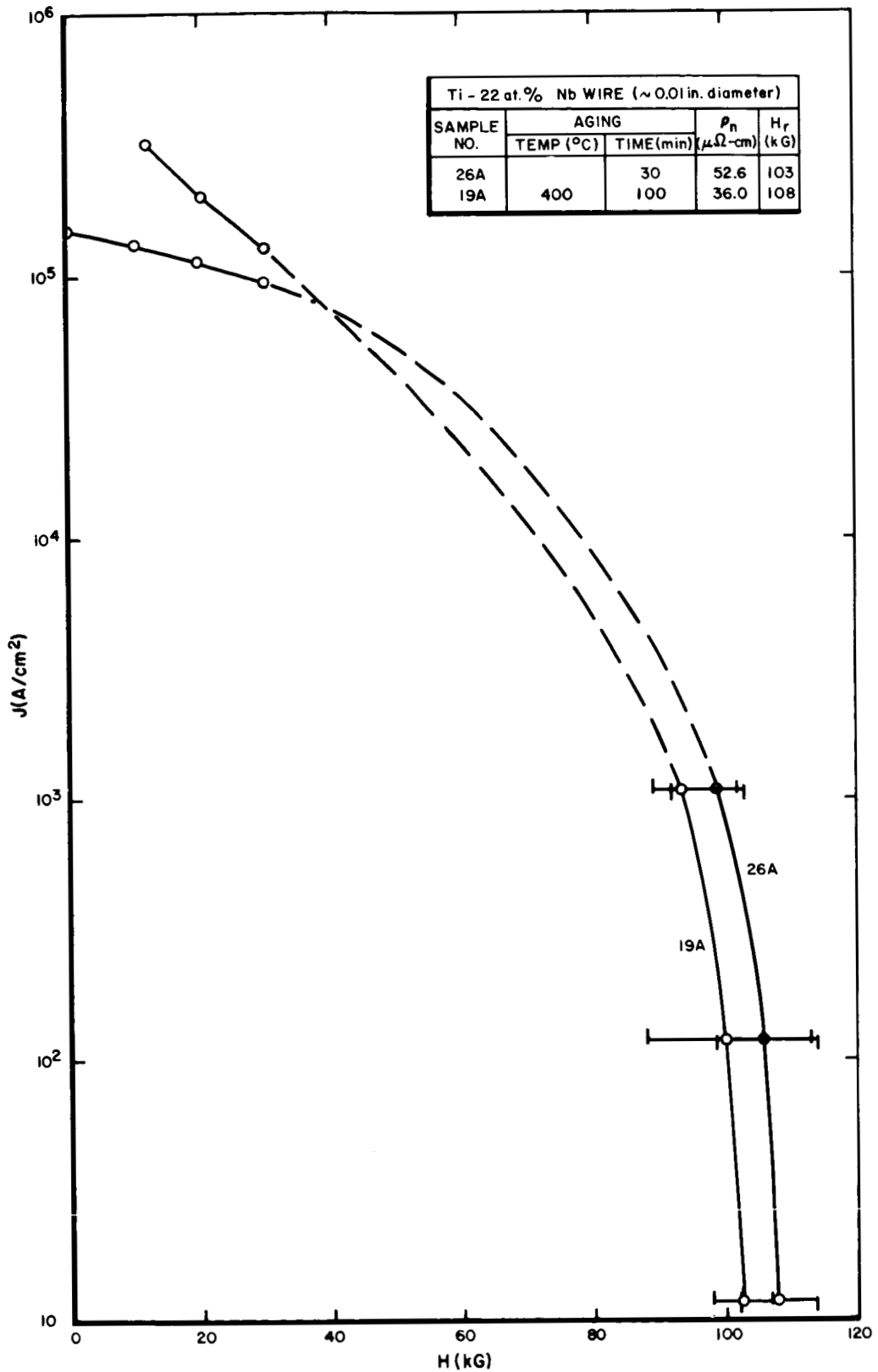


Figure 6. Critical Current Density and Resistive Upper Critical Field at 4.2°K for 0.01-in. -Diameter Ti-22 a/o Nb Wire Annealed at 400°C for the Times Shown

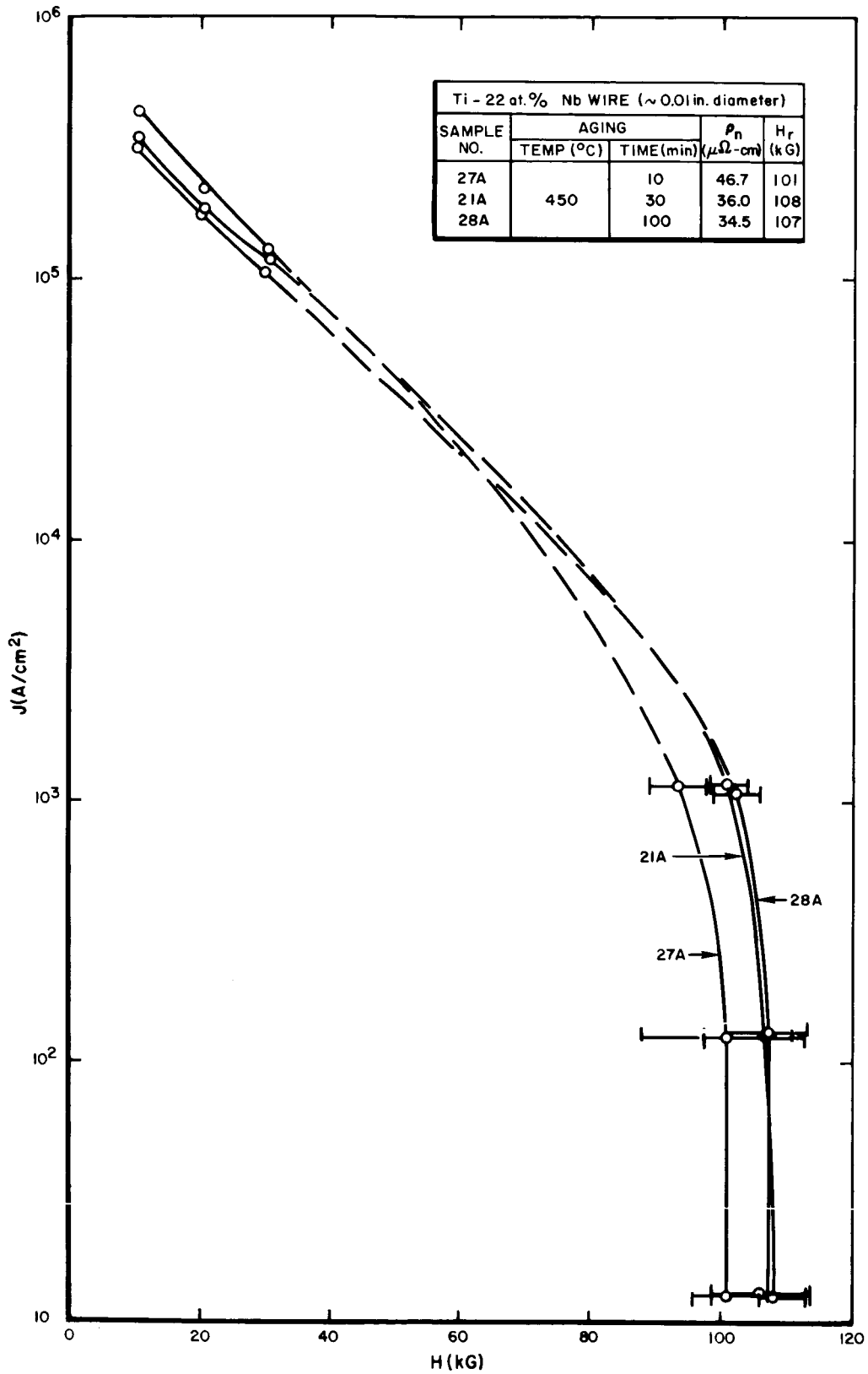


Figure 7. Critical Current Density and Resistive Upper Critical Field at 4.2°K for 0.01-in.-Diameter Ti-22 at.% Nb Wire Annealed at 450°C for the Times Shown

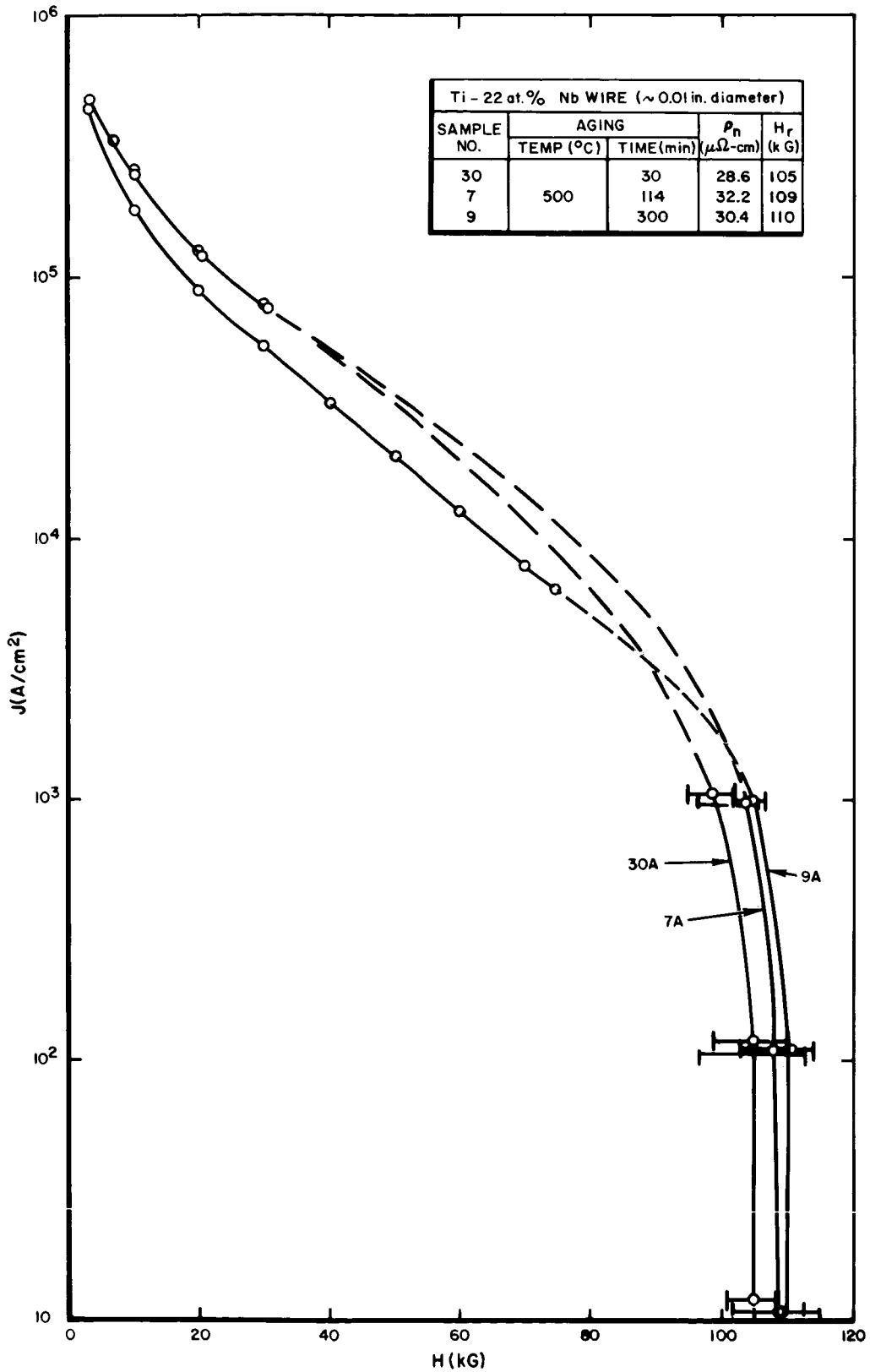


Figure 8. Critical Current Density and Resistive Upper Critical Field at 4.2°K for 0.01-in.-Diameter Ti-22 at.% Nb Wire Annealed at 500°C for the Times Shown

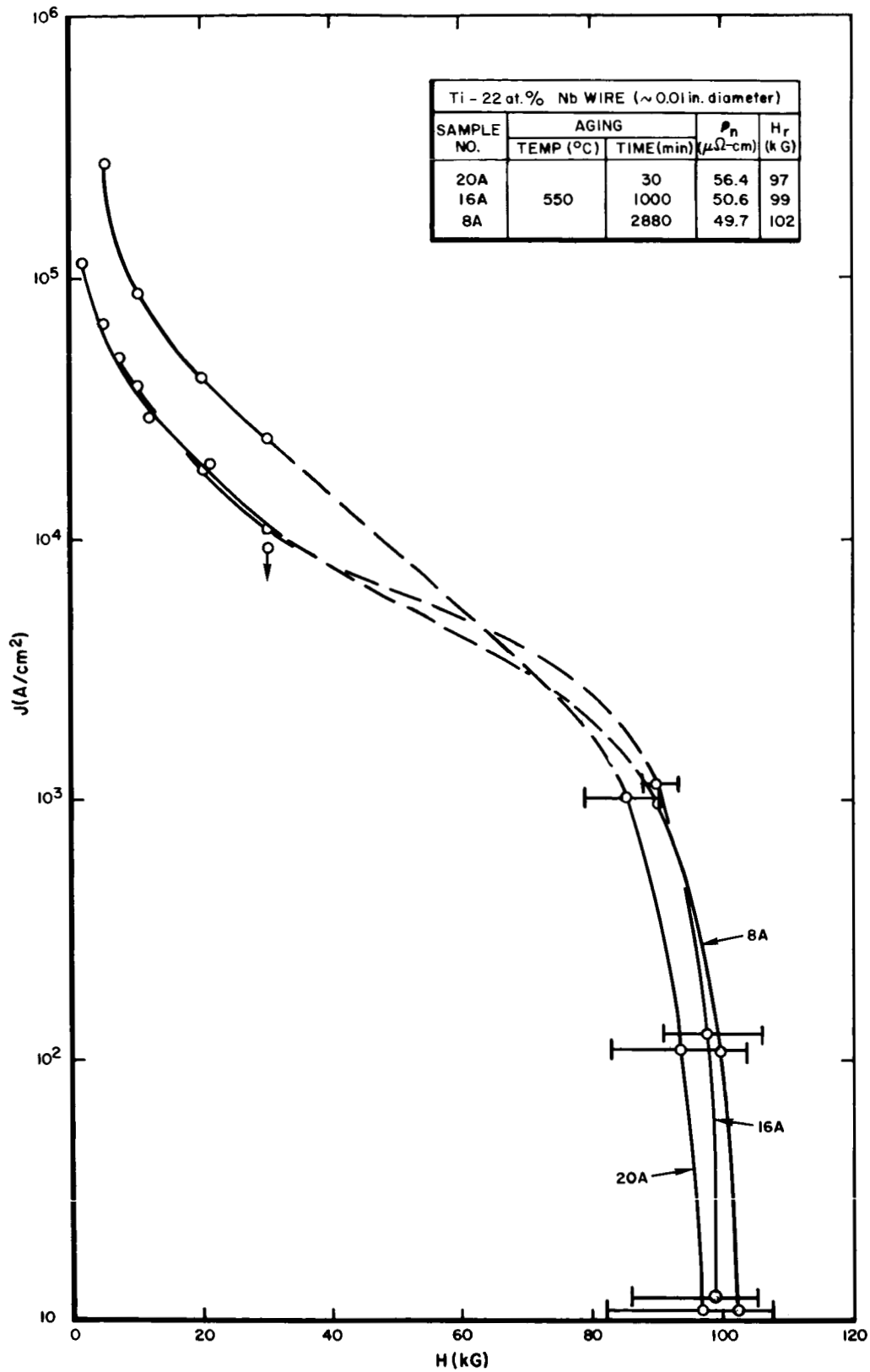


Figure 9. Critical Current Density and Resistive Upper Critical Field at 4.2°K for 0.01-in.-Diameter Ti-22 at.% Nb Wire Annealed at 550°C for the Times Shown

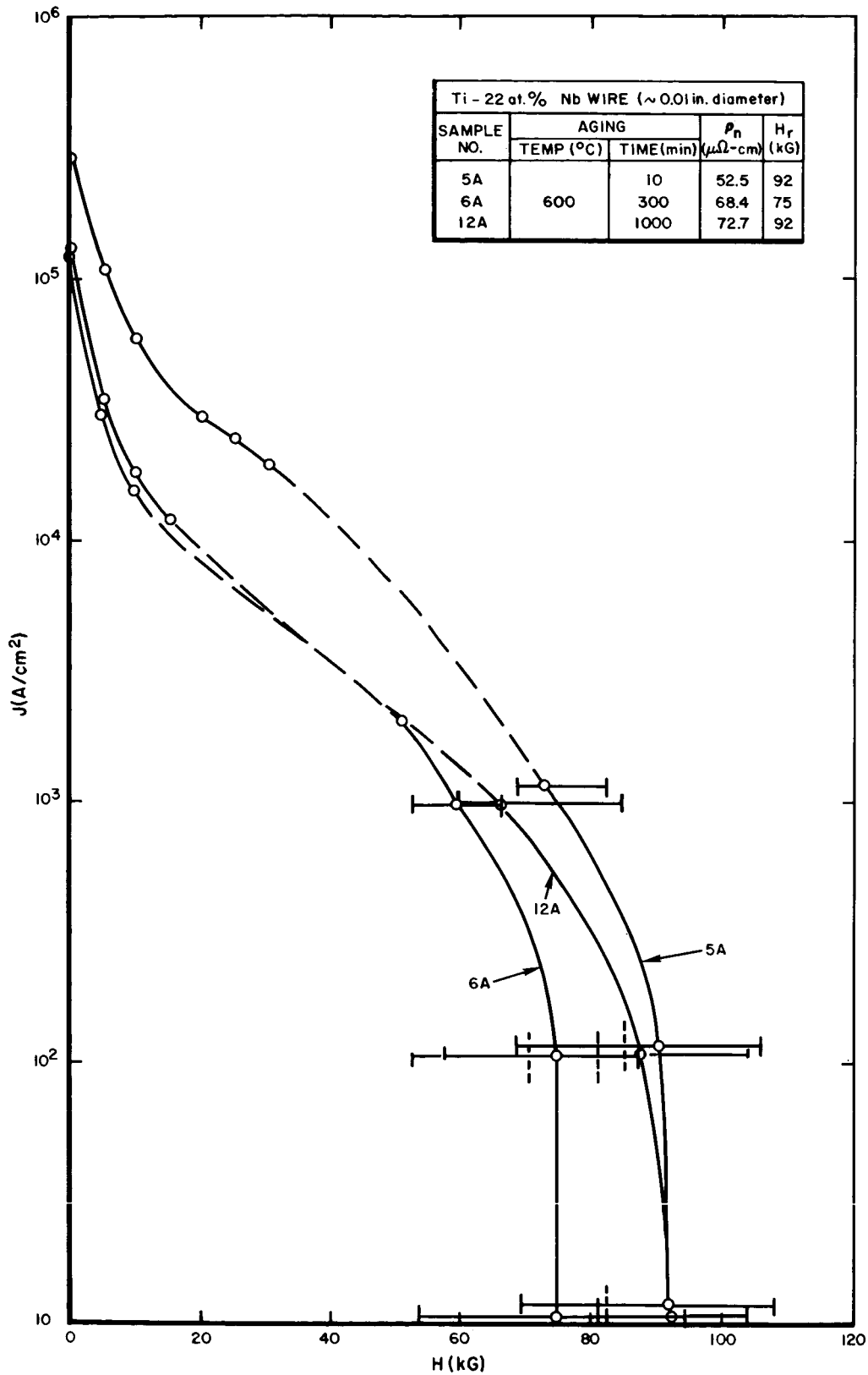


Figure 10. Critical Current Density and Resistive Upper Critical Field at 4.2°K for 0.01-in.-Diameter Ti-22 at.% Nb Wire Annealed at 600°C for the Times Shown

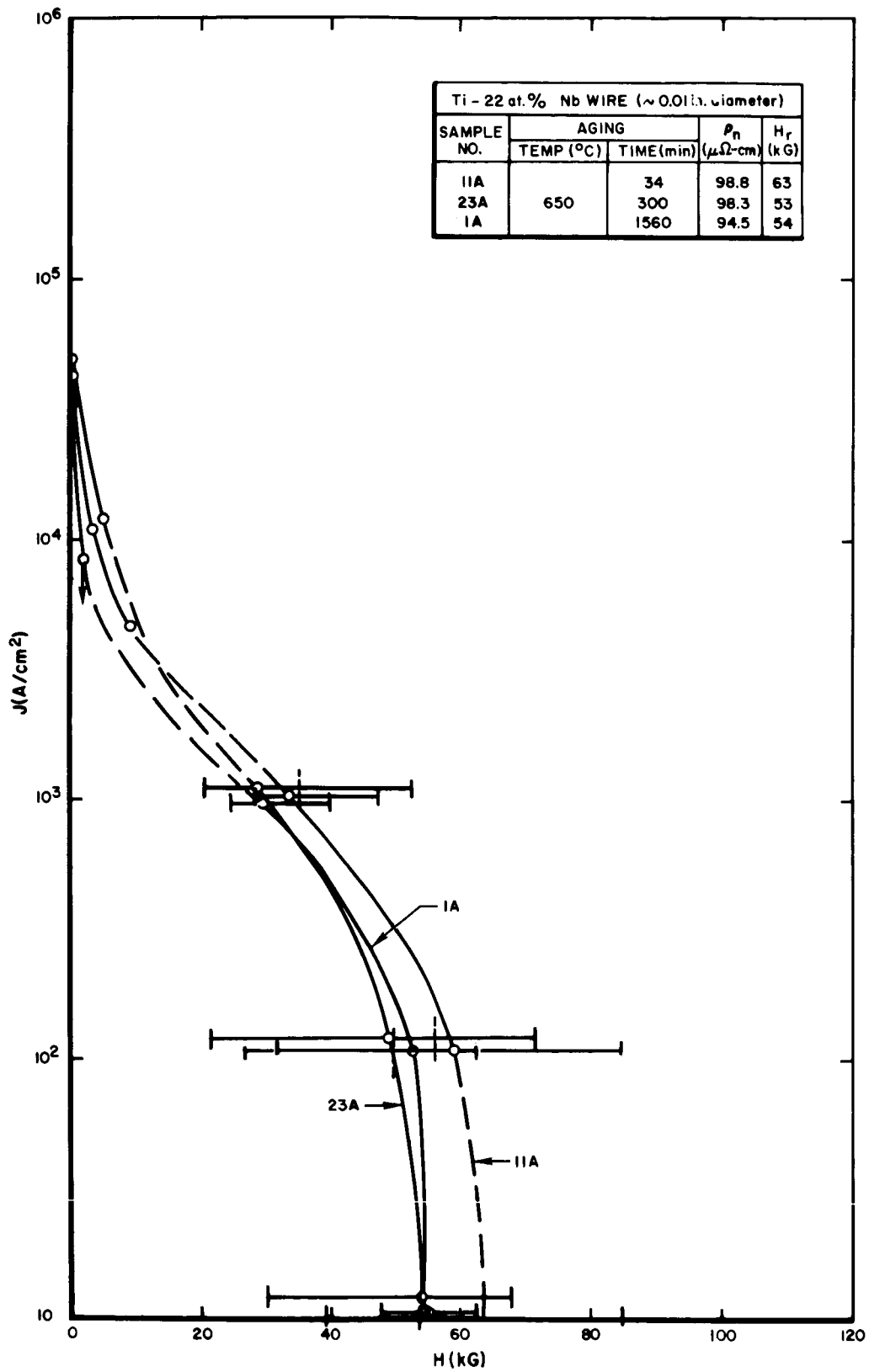


Figure 11. Critical Current Density and Resistive Upper Critical Field at 4.2°K for 0.01-in. -Diameter Ti-22 a/o Nb Wire Annealed at 650°C for the Times Shown

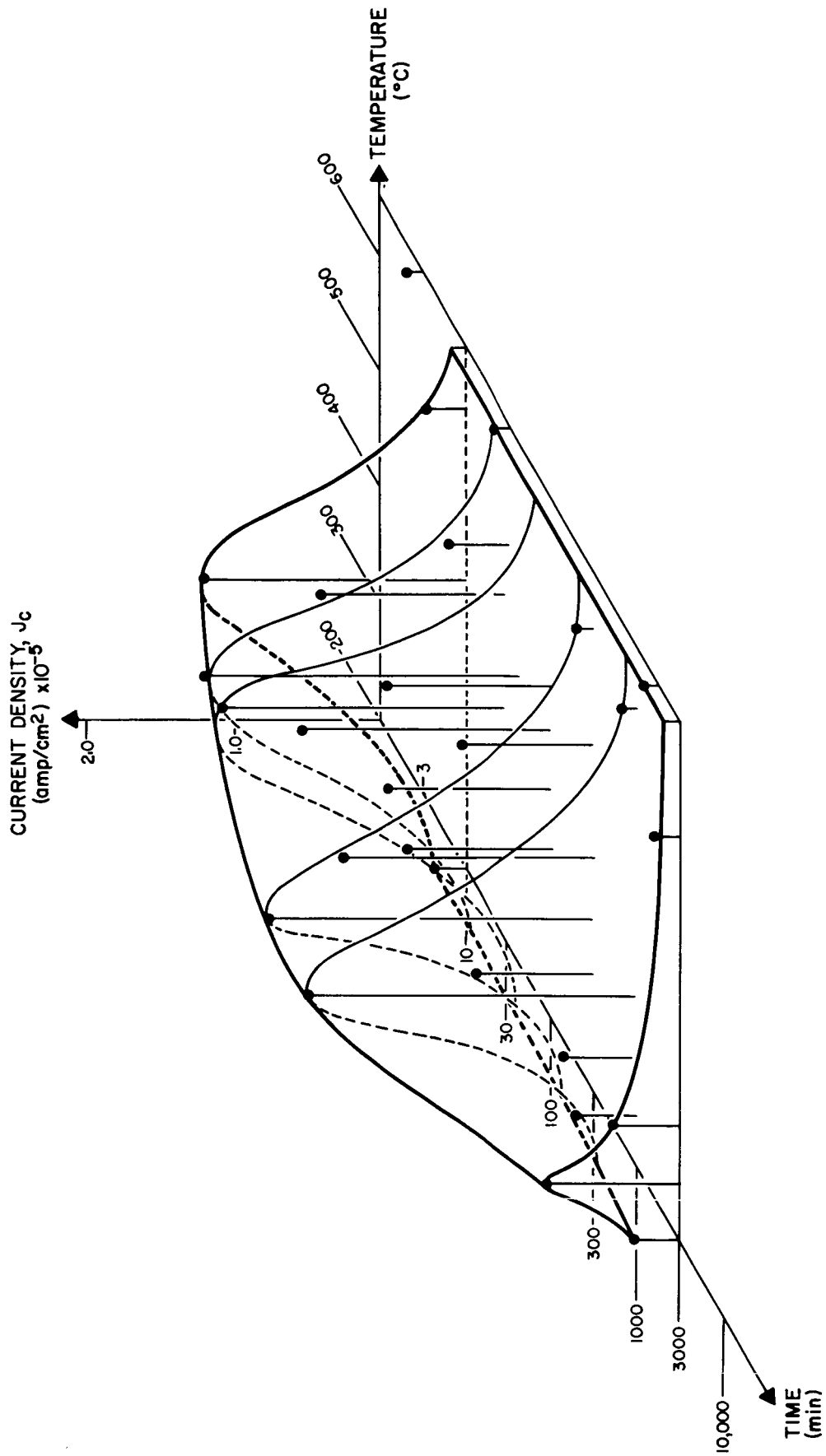


Figure 12. Isometric Graph of 4.2° K Critical Currents at 30 kG for Ti-22 ^a/_o Nb as a Function of Annealing Temperature and Time

III. RESISTIVE UPPER CRITICAL FIELD MEASUREMENTS

A. DESCRIPTION

The resistive upper critical fields, H_{r} , for the 30 Ti-Nb wire samples have been measured using pulsed-field techniques. In this method, a transverse sample is tested in a pulsed-field solenoid. The experimental sequence is the following: a small sample current is established in zero field, then the solenoid field is increased with ms. rise times and a voltage is observed across the sample. The voltage results from a super-to-normal (SN) transition at the critical field of the test sample. As the pulsed-field decays, the sample undergoes a normal-to-super (NS) transition provided the transport current was not sufficient to cause propagation of the normal region. The SN and NS transitions are not abrupt in Type II superconductors, but take place over several kilogauss, even for homogeneous samples.

The experimental circuitry is illustrated in Figure 13.

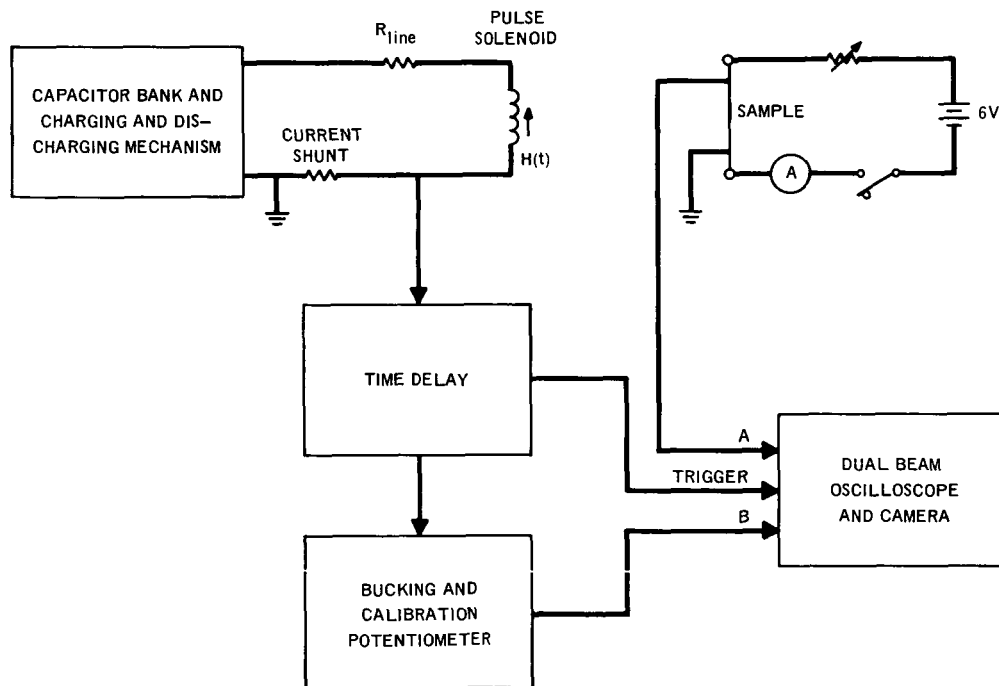


Figure 13. Experimental Circuitry, H_r Measurements

The pulsed magnet current (field) and sample voltage are recorded with an oscilloscope. The time delay is used to trigger the sweep just prior to the SN transition, thereby permitting expanded sweeps of the transition voltage and field. The bucking potentiometer subtracts a fixed voltage across the solenoid current shunt for higher field recording sensitivity.

Two pulses are recorded on each photograph: one with sample current flowing to record the SN transition, and the second with no sample current to measure the noise level due to $d\phi/dt$ pickup. A typical pulse is shown in Figure 14a. The repeatability of the pulse is evident since the two solenoid field traces are identical. Both the SN transition and the NS transition are well defined.

Data were taken at current levels of 0.005, 0.05, and 0.5A, corresponding to approximately 10, 100, and 1000 A/cm², respectively. At each current level two pictures were taken: one showing both SN and NS transitions, and a second showing an exploded view of the SN transition.

The SN transition occurs at consistently higher fields than the NS transition. Evidently this discrepancy results from eddy current heating in the sample due to $d\phi/dt$, thus the SN transition is more correct. From the above discussion, it follows that $d\phi/dt$ must also cause H_r for the SN measurement to be less than H_{c2} , the upper critical field.

In analyzing the data, three to four fields are noted. H_r is defined as the field at which half of the normal-state resistance is restored. The fields at which the onset and full restoration of resistance occur are labeled H_{ro} and H_{rf} , respectively. In some cases a double transition is evident, as shown in Figure 14b. The field at which the second transition begins is labeled H'_{ro} .

The data are plotted in Figures 1 through 11. Each graph shows the results for wires annealed at the same temperature for different times. The data points represent H_r , while the bars indicate H_{ro} and H_{rf} . If the sample has a double transition, H'_{ro} is represented with a dashed, vertical line. The values of H_r for the samples are plotted as a function of annealing temperature in Figures 15a and 15b, and as a function of annealing time in Figure 16.

Often, at current densities of $\sim 10^3$ A/cm², normal regions propagate along the wire; a typical result is shown in Figure 13c. In this figure, the sample voltage (V_s) increases abruptly as the normal region propagates past one voltage

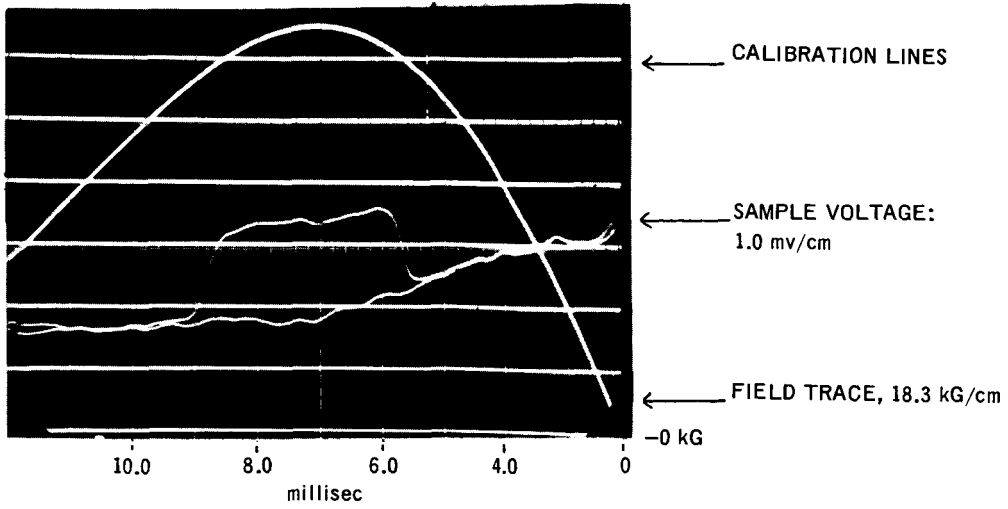


Figure 14a. Typical SN Transition in Pulsed-Field, Sample No. 9, $J = 109 \text{ A/cm}^2$

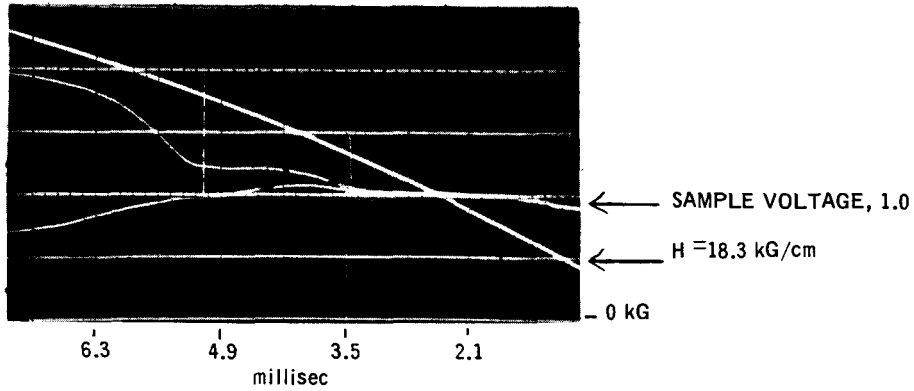


Figure 14b. Double Transition in Sample No. 5, $J = 117 \text{ A/cm}^2$

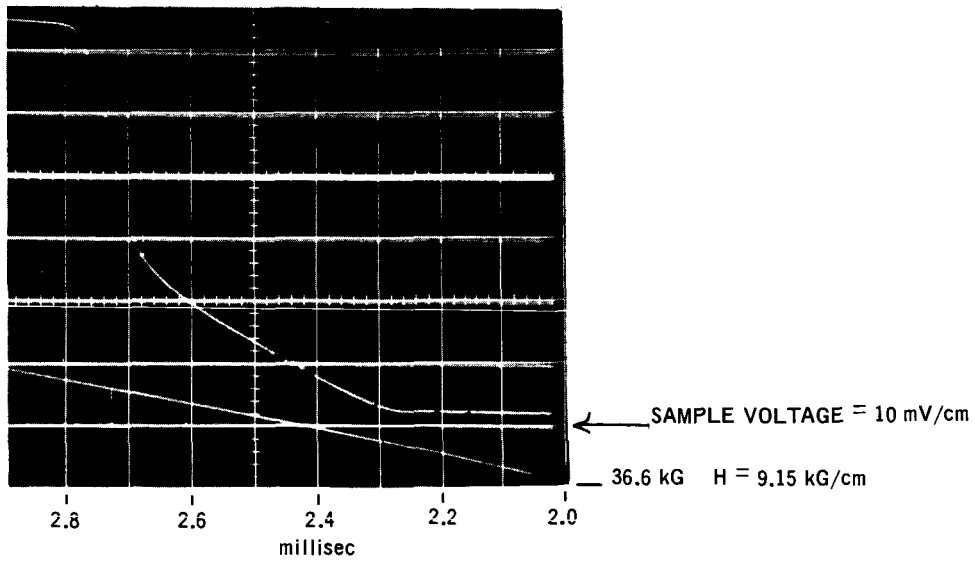


Figure 14c. Propagation of Normal Region Originating in Solder Joints

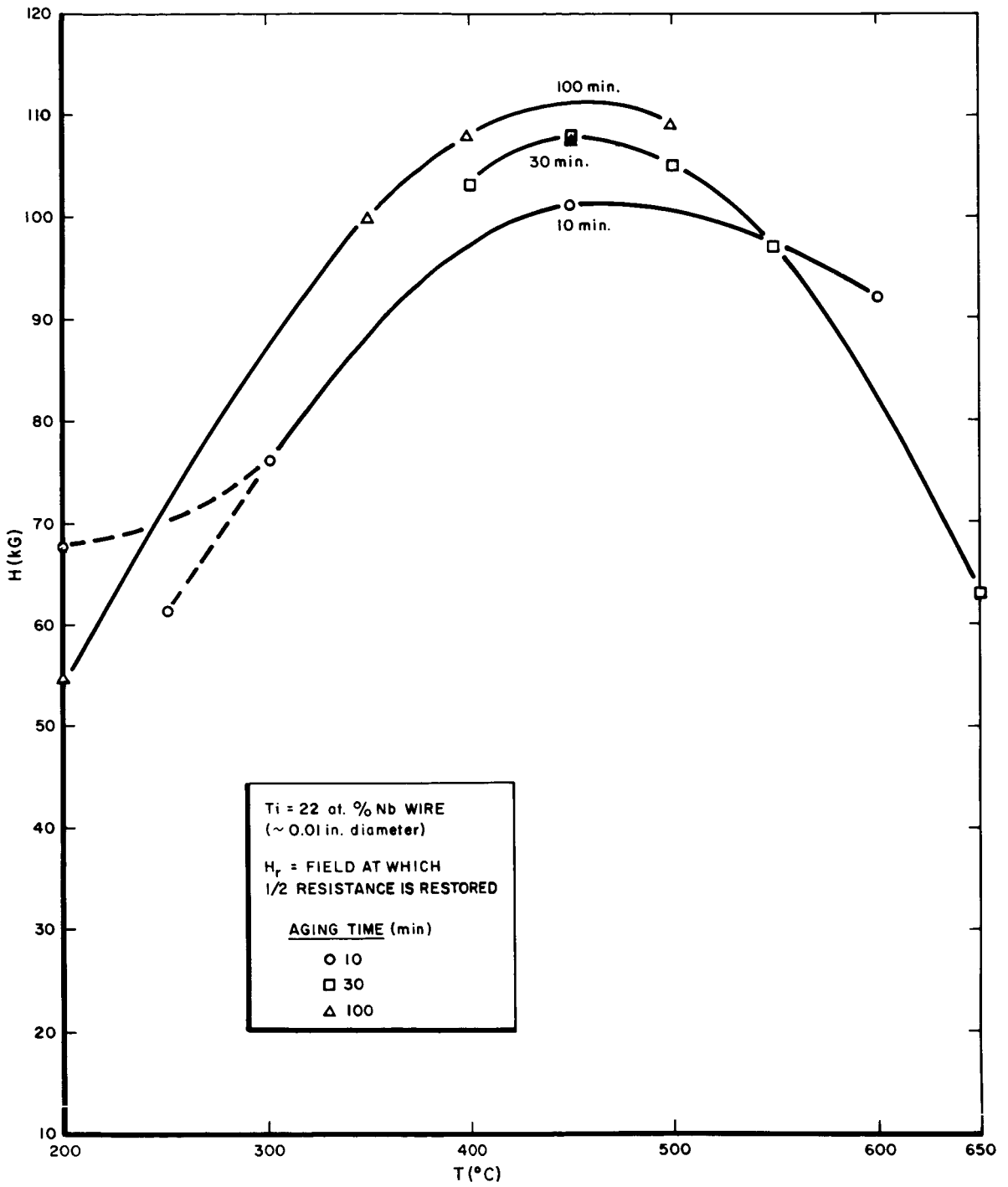


Figure 15a. Resistive Upper Critical Field at 4.2°K of Ti-22 at. % Nb as a Function of Annealing Temperature, for Different Annealing Times

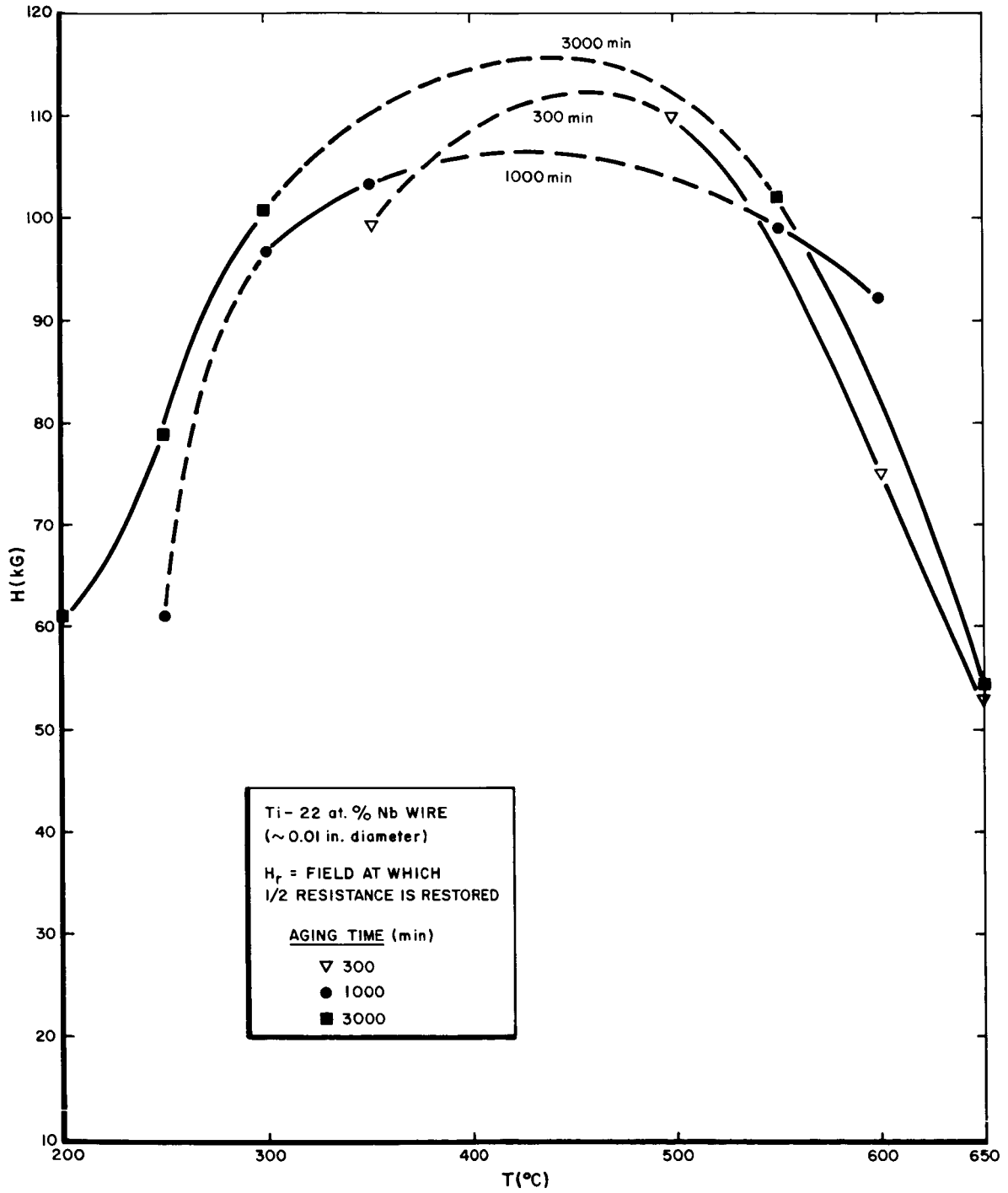


Figure 15b. Resistive Upper Critical Field at 4.2°K of Ti-22 at.% Nb as a Function of Annealing Temperature, for Different Annealing Times

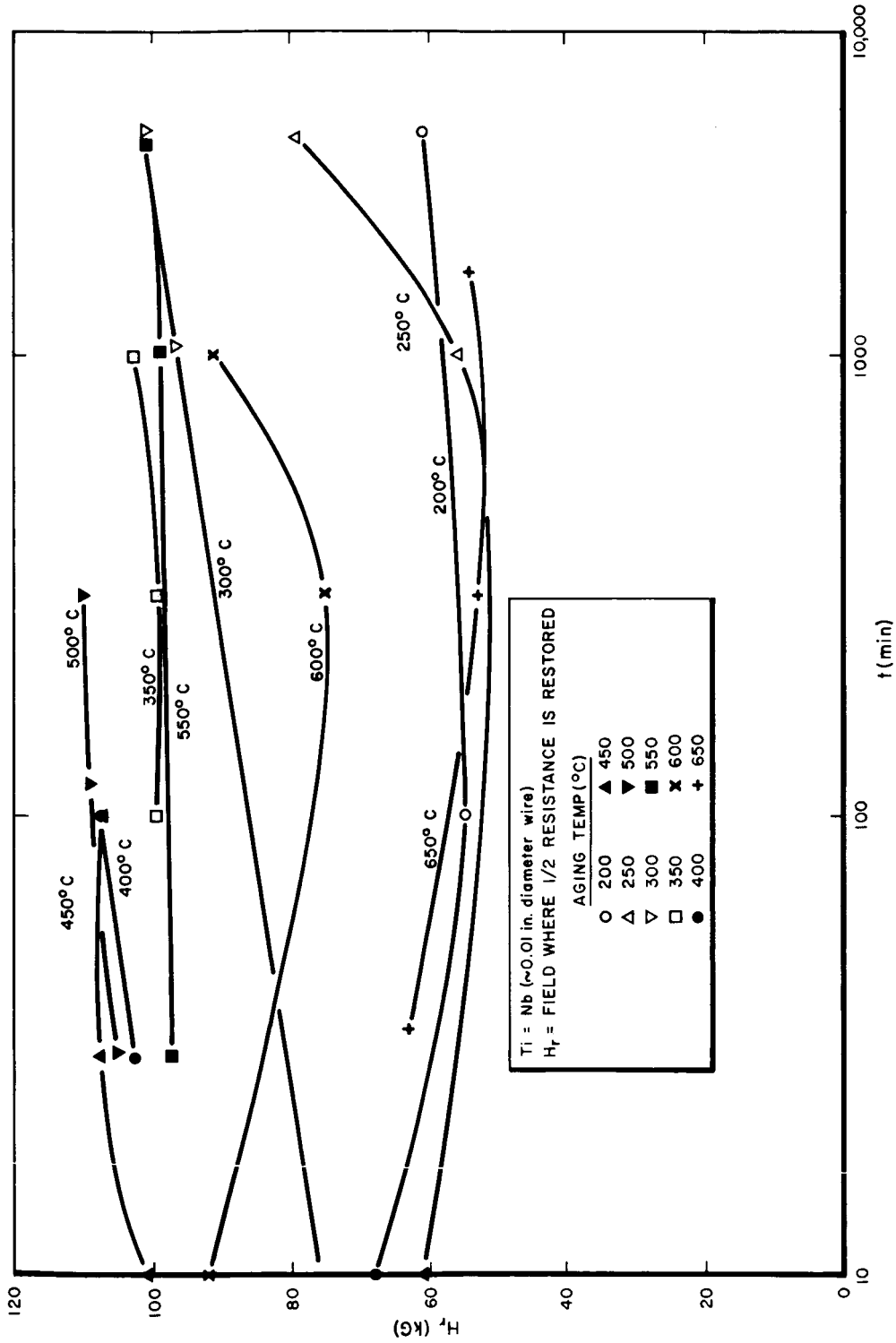


Figure 16. Resistive Upper Critical Field at 4.2°K of Ti-22 ^a/_o Nb as a Function of Annealing Time, for Different Annealing Temperatures

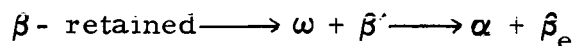
probe. If H were constant, V_s should increase linearly.⁽¹⁾ However, since H is increasing, d^2V_s/dt^2 should be positive, which is the case. The average propagation velocity (ignoring the change in H) is reasonable, about 4 m/sec. The initial normal region evidently results from heating at the solder joints between the sample and the current leads and propagates if the current density is large enough.

From Figure 14c, the expected SN transition occurs at ~ 0.7 ms, a time too short to be due to a propagating normal front from the joints. Therefore, the magnetic SN transition is a true measure of the upper resistive critical field.

B. DISCUSSION

Changes in H_r can be tentatively explained as follows. Figure 17 shows a portion of the equilibrium phase diagram for Ti-Nb, and Figure 18 shows H_r (at 1.2°K) from homogeneous Ti-Nb.^(2,3) The starting material is quenched from 800°C and has a homogeneous, retained- β structure. From Figure 17, it is seen that if retained- β is annealed at $T \leq 680^\circ\text{C}$, then αTi is precipitated: the matrix material ($\beta\text{-Nb}$) surrounding the precipitate becomes enriched in Nb. Thus the matrix composition is changed, and H_r should change in accord with Figures 17 and 18.

Quantitative confirmation of this process must await critical temperature determinations for the 30 samples because our data was taken at 4.2°K and Figure 17 was taken at 1.2°K.* This difficulty can be evaded in one specific case by comparing the results at the maximum value of H_r . From Figures 15a and 15b, H_r is maximum at $\sim 450^\circ\text{C}$. From Figure 17, the equilibrium β -phase for a 450°C anneal should be 50^a/o Nb. However, the maximum value of H_r from Figure 18 occurs for 40^a/o Nb. This apparent discrepancy in Nb concentration might be explained as follows: the kinetics of the Ti-Nb alloy system indicate a sluggish transformation with precipitation of a transient ω -phase.⁽⁴⁾



The intermediate β phase could be of lower Nb concentration, that is substantial 40^a/o Nb could be present for material which finally becomes 50^a/o Nb.

*If the composition is ≤ 40 ^a/o Nb, then $^3H_r = 18,400 T_c [1 - (T/T_c)^2]$

If the composition is ≥ 40 ^a/o Nb, $H_r = A(T) \rho n \gamma T_c [1 - (T/T_c)^2]$

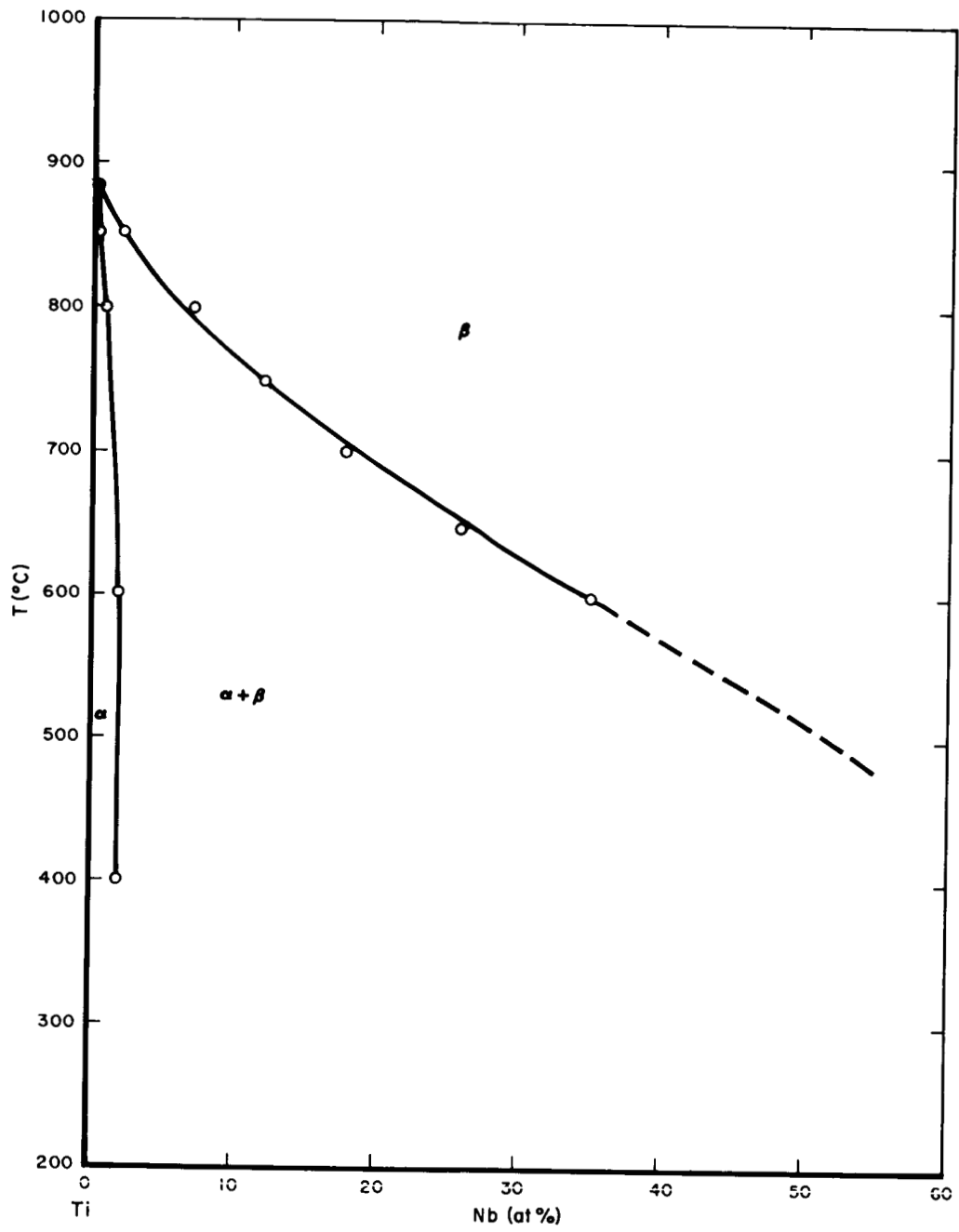


Figure 17. Ti-Nb Phase Diagram

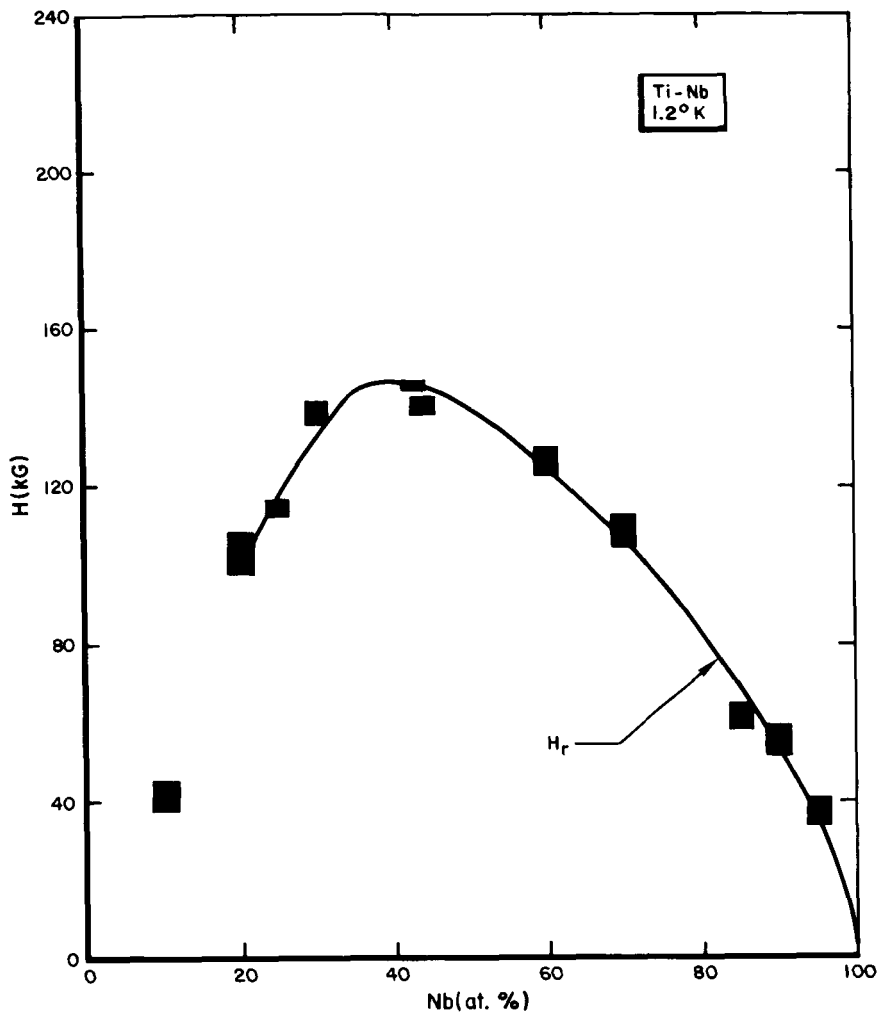


Figure 18. Upper Critical Field of Ti-Nb at 1.2°K as a Function of Alloy Concentration

In the samples aged at 600 and 650°C, broad double SN transitions of 30-kG width were observed (see Figures 10 and 11). A typical photograph of this broad double transition is shown in Figure 14b. This result is not understood as yet, but it is thought to be due to the α -Ti precipitate. Double transitions, such as illustrated in Figure 12c, are seen in most of the broad transitions.

We thank Dr. A. C. Thorsen for his cooperation and the use of the pulse-solenoid facilities at the North American Science Center.

IV. NORMAL STATE RESISTIVITY

Resistivity measurements were made at room temperature on the pre- and post-annealed material (ρ_o and ρ_f , respectively). The normal-state resistivity at 4.2°K (ρ_n) was calculated from the voltage and current measurements in the pulsed-field tests at 10^3 A/cm². The results are given in Table 1. From the ρ_n data, it is seen that a low value of ρ_n corresponds to a high H_r . Since, from the preceding section, high H_r corresponds to an enriched Nb phase, and since ρ_n decreases with increasing Nb content,⁽³⁾ the above results are expected.

TABLE 1
CRITICAL CURRENT, NORMAL STATE RESISTIVITY, AND HARDNESS OF
Ti-22 at. % Nb ALLOY FOR VARIOUS ANNEALS

Sample	Annealing Parameters		As-Drawn, 22°C Resistivity ρ_0 ($\mu\Omega$ -cm)	Post-Anneal, 22°C Resistivity ρ_f ($\mu\Omega$ -cm)	Normal State, 4.2°K Resistivity ρ_n ($\mu\Omega$ -cm)	Hardness (KHN)	Critical Current Density at 20 kG J_c (amp/cm ²) $\times 10^{-4}$
	Time (minutes)	Temperature (°C)					
1	3,000	650	117	108	94.5	216	<1.0
2	10	200	110	107	94.0	241	2.2
3	3,000	250	116	88	54.8	480	9.6
4	1,000	250	117	105	84.5	426	4.0
5	10	600	115	85	52.5	226	2.9
6	300	600	113	88	68.4	236	<1.0
7	100	500	117	72	32.2	211	12.0
8	1,000	550	121	77	49.7	207	†
9	300	500	119	71	30.4	282	9.0
10	3,000	200	117	107	90.2	395	3.3
11	30	650	115	113	98.8	234	<1.0
12	1,000	600	115	90	72.7	†	<1.0
13	1,000	300	116	82	41.4	423	5.2
14	1,000	350	113	68	29.0	409	23.8
15	3,000	300	112	69	33.6	207	4.4
16	3,000	550	112	75	50.6	†	1.8
17	100	350	112	75	41.4	423	10.0
18	10	250	116	103	97.2	382	†
19	100	400	113	71	36.0	423	11.5
20	30	550	112	77	56.4	253	4.1
21	30	450	114	66	36.0	†	28.5
22	300	350	115	59	50.0	454	23.0
23	3	650	111	70	98.3	†	<1.0
24	10	300	111	81	67.1	†	8.2
25	30,000	200	†	†	87.2	†	3.9
26	30	400	118	78	52.6	370	20.0
27	10	450	120	79	46.7	359	18.6
28	100	450	120	71	34.5	347	17.5
29	300	400	119	67	†	†	18.0
30	30	500	115	68	28.6	†	13.2
800*			113	†	105	282	5.0

*This sample represents the cold-worked state of the as-drawn 10-mil wire.

†Data not available at this writing.

V. SUMMARY AND FUTURE PLANS

Short sample J_c vs H and H_r tests are complete. At 4.2°K in a field of 30 kG, the maximum in critical current density, 2×10^5 A/cm², is found for material which is annealed 300 to 1000 minutes at 350°C. The resistive upper critical field, H_r , is maximum for a 100 to 300 minute, 450°C anneal. Variations in H_r due to annealing can be qualitatively explained by identifying with a precipitation-enriched, β -Nb matrix. Quantitative correlation will be made after critical temperature experiments are complete.

Continuing, but incomplete, work includes photomicrograph, x-ray diffraction, and electron microscope studies on the annealed wire.

New experiments scheduled for the third quarter include critical temperature and short sample stability tests for the 30 samples.

REFERENCES

1. C. N. Whetstone, "Thermal Phase Transitions in Superconducting Nb-Zr Alloys," Ph.D. Thesis, Vanderbilt University (1964)
2. M. Hansen, et al., Trans. Am. Inst. Mining Met. Engrs., 191, 881-888, (1951)
3. T. G. Berlincourt and R. R. Hake, Phys. Rev. Letters, 9, 7 (1962)
4. J. B. Vetrano, private communication